BIOCYBERNETICS AND BIOMEDICAL ENGINEERING 37 (2017) 326–335

Available online at www.sciencedirect.com

ScienceDirect

journal homepage: www.elsevier.com/locate/bbe

Original Research Article

# Comparative evaluation of EMG signal features for myoelectric controlled human arm prosthetics

*Derya Karabulut* [a], *Faruk Ortes* [b], *Yunus Ziya Arslan* [b,*], *Mehmet Arif Adli* [c]

[a] *Department of Mechanical Engineering, Faculty of Engineering, Haliç University, Istanbul, Turkey*
[b] *Department of Mechanical Engineering, Faculty of Engineering, Istanbul University, Istanbul, Turkey*
[c] *Department of Mechanical Engineering, Faculty of Engineering, Gazi University, Ankara, Turkey*

ARTICLE INFO

*Article history:*
Received 28 October 2016
Accepted 20 March 2017
Available online 31 March 2017

*Keywords:*
Electromyography
Prosthetics
Feature
Classification
Prediction

ABSTRACT

Myoelectric controlled human arm prosthetics have shown a promising performance with regards to the supplementation of the basic manipulation requirements for amputated people over recent years. However these assistive devices still have important restrictions in enabling amputated people to perform rather sophisticated or functional movements. Surface electromyography (EMG) is used as the control signal to command such prosthetic devices to ensure the amputated people to compensate their fundamental movement patterns. The ability of extraction of clear and certain neural information from EMG signals is a critical issue in fine control of hand prosthesis movements. Various signal processing methods have been employed for feature extraction from EMG signals. In this study, it was aimed to comparatively evaluate the widely used time domain EMG signal features, i.e., integrated EMG (IEMG), root mean square (RMS), and waveform length (WL) in estimation of externally applied forces to human hands. Once the signal features were extracted, classification process was applied to predict the external forces using artificial neural networks (ANN). EMG signals were recorded during two types of muscle contraction: (i) isometric and isotonic, and (ii) anisotonic and anisometric contractions. Experiments were implemented by six healthy subjects from the muscles that are proximal to the upper body, i.e., biceps brachii, triceps brachii, pectoralis major and trapezius. The force prediction results obtained from the ANN were statistically evaluated and, merits and shortcomings of the features were discussed. Findings of the study are expected to provide better insight regarding control structure of the EMG-based motion assistive devices.



## 1. Introduction

Electromyography (EMG) signal is the electrical manifestation of a contracting muscle that is the most important indicator of the muscle performance associated with neuromuscular activation during muscle contraction [1]. EMG is also a crucial concept to understand the relationship between muscle activation and limb motions. Surface EMG signal is the non-invasively recorded form of muscle activity and has been

* *Corresponding author at*: İstanbul Üniversitesi, Mühendislik Fakültesi, Makine Mühendisliği Bölümü, 34320 Avcılar, İstanbul, Turkey.
E-mail addresses: deryakarabulut@halic.edu.tr (D. Karabulut), faruk.ortes@istanbul.edu.tr (F. Ortes), yzarslan@istanbul.edu.tr (Y.Z. Arslan), arif.adli@gazi.edu.tr (M.A. Adli).
http://dx.doi.org/10.1016/j.bbe.2017.03.001
0208-5216/

widely applied to increase the motion capability of the human arm prosthetics [2–4]. For the people subjected to the lower or upper limb amputations such as transhumeral or transradial ones, prostheses became one of the most critical issues in terms of patients' vital functional requirements and cosmetic concerns. EMG-based human arm prosthesis are developed to compensate the lost function of amputated people by using EMG data of residual limbs as control signals to perform a corresponding motion for the prosthesis. Over the last three decades, extensive research has been developed on the EMG controlled prostheses for both upper-limb [5–8] and lower limb [9–11] amputations. Dexterous control of powered human arm prostheses highly depends upon a well-defined relationship between EMG signals and externally exerted forces to execute a variety of forces as performing different limb motions [12–14].

Feature extraction from biological signals is a process to obtain the useful information from raw signal in a condensed form which is intended to use for specific applications such as prosthetic control, diseases diagnosis and motion pattern recognition [15]. Since the main assumption of pattern recognition of SEMG is that each task is characterized by a set of signal features, which implies muscle activation [3], the techniques used for obtaining features play a critical role in representing the neuromuscular activity of muscles during different kinds of contractions. EMG signal characteristics are identified using features in time, frequency or time-frequency domains [16]. To analyze and classify the user's motion intention, the time domain features are commonly accepted as usable properties [17,18]. Since time domain features do not need any domain transformation due to raw EMG signal recorded over time scale, the features evaluated in time domain require remarkably less time for calculation, thereby leading to faster online control of prosthetics [15,16,19].

For the position or force control of a prosthetic device, extracted signal features are needed to be classified using various machine learning systems. The recognized EMG patterns are considered to reflect the users' motion intentions. These reduced and classified signals are fed into the control scheme of the prosthetics as command signal [16]. A considerable amount of research has been published on pattern recognition methods and applications which provide better decoding of EMG signals [16,19–22]. A group of techniques has been proposed for pattern recognition such as support vector machines (SVM) [23–25], linear discriminant analysis (LDA) [26,27], fuzzy logic [20,28,29] and artificial neural networks (ANN) [19,30–32]. Due to the prominent performance in classification of EMG features and the capability of predicting time-varying targets, ANN was found the most extensive application area among these techniques [2,6,19].

In pattern recognition process, previous studies highlighted the success of neural networks to classify implementation of tasks by taking advantage of the ability to represent both linear and nonlinear relationships [16]. Hiraiwa et al. obtained motion patterns of flexor digitorium superficialis performing neural networks [33] and Hudgins et al. applied ANN to classify time domain features for EMG based prostheses [19]. Prediction of externally applied forces and torques using neural networks has a key role to contribute artificial human limbs [5,13,14,34]. Morita et al. proposed a control method for human hand prosthesis that could estimate joint torque from EMG signals [5].

The objective of the study was to establish a relationship between EMG signals and externally applied forces which can be used in force control scheme of the myoelectric based prosthesis. To be able to achieve this goal, EMG signals were recorded under different contractile and loading conditions, and time domain features of these signals were extracted, i.e., root mean square (RMS), integrated EMG (IEMG) and waveform length (WL). Obtained features were classified using ANN to predict the externally applied forces to human hands. In final stage, performance of the features in terms of representing the user's force intensions was comparatively evaluated.

## 2. Materials and methods

### 2.1. *Experimental procedure and EMG signal acquisition*

EMG signals supplied to pattern recognition process were recorded during two different types of muscle contractions. A series of experiments were performed to obtain the myoelectric signals during (*i*) isometric and isotonic, and (*ii*) anisotonic and anisometric contractions. Experiments were performed by six healthy subjects who are right-handed and in a range of 25–35 year-old aging. SEMG recording processes were carried out for 3 subjects in isometric contraction, while for other 3 subjects in anisometric contraction. Before the signal recording process, subjects were given sufficient information about the experiments and their informed consents were taken. All EMG measurement protocol was carried out recording to the recommendation of SENIAM Project [35].

The basic idea of myoelectric controlled prosthesis is to provide the control signal from the electrical activity of residuals muscles residing in the proximal part of upper human trunk. Therefore, in the experimental protocol, SEMG data were recorded simultaneously from muscles including biceps brachii, triceps brachii, pectorialis major and trapezius.

Since the EMG signal is of a stochastic characteristics rather than a deterministic behavior, and is highly sensitive to the environmental effects, it is almost impossible to acquire the same EMG signal for the same motion even from the same subject under the same contractile conditions. The complex structure of EMG signals requires subject-specific control process designs for each amputee's myoelectric arm. Therefore, in this study, instead of recruiting a high number of subjects, which leads to a great burden of data set, it was preferred to record many EMG data for different contractile conditions from a condensed set of subjects. By doing so, we were able to focus our attention on consistent and reliable force prediction from EMG signals specific to the each individual. In total, 350 different trials for isometric case and 40 for anisometric case were performed by each subject.

### 2.2. *Isometric contraction experiments*

As a first step for investigation of muscle activation, isometric contraction experiments have been performed. The relation between muscle activity at constant length and externally applied forces were focused during the following experimental procedures.

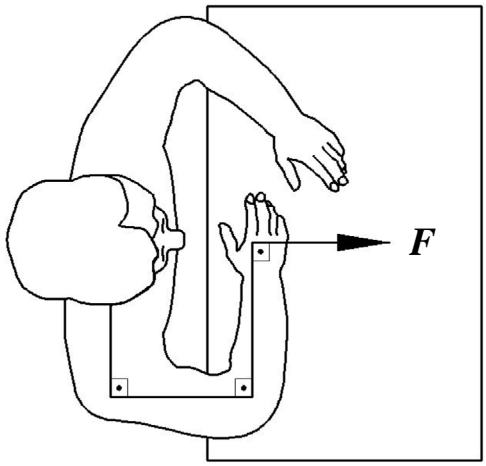


**Fig. 1 – Top view of experimental set-up for isometric contractions.**

The subject's right forearm positioned on a glass surfaced table parallel to coronal plane and was stabilized at flexed position of 90° while the forces were applied (Fig. 1). The abduction and flexion angles of right upper arm were 0° and 45°, respectively. Furthermore, a special silk fabric with low dry friction placed between the skin surface of the forearm and the table, to reduce the dry friction. Different force amplitudes from 10 N to 70 N with 10 N increments were externally applied to human hands during experiments. Each trial of isometric contraction was taken for 3 s and 50 trials were recorded for each force level, that is, totally $50 \times 70 = 350$ trials were recorded for each subject.

The position of shoulder and arm was stationary during experiments. The force direction was perpendicular to the longitudinal axis of the forearm (Fig. 1).

Furthermore, sufficient duration of time was allocated for resting of subjects between each successive measurement to avoid muscle fatigue that may potentially leads to uncertainties on signal characterization [36].

EMG recording system used in the experiments is Key Point version 5.03, Physiomed, Denmark (common mode rejection ratio > 100 dB, input impedance: 1000 M, signal to noise ratio = 0.6 V). Ag/AgCl disk electrodes with 10 mm diameter were employed for EMG recordings. To reduce the motion artifacts and to ensure a good contact between the electrodes and skin surface, alcohol was used to clean the skin surface and a special conducting gel was applied. The sampling frequency of the signals was 500 Hz. A bandpass filter with 20 Hz lower and 250 Hz upper cut-off frequencies was applied.

### 2.3. *Anisometric contraction experiments*

Anisometric contraction experiments, which include length change of muscles during exerting time-varying forces, were performed according to following considerations. A SCARA type robot with 3 degrees of freedom, consisting of three limbs that are connected by rotational joints to each other, was operated to supply resistive forces against human arm tips for anisometric contractions (Fig. 2a). A handle bar at the tip of the manipulator was kept by the subjects during experiments (Fig. 2b). Furthermore, two six-axis force/torque sensors (NITTA Corporation, Japan, 500 Hz sample frequency, accuracy ±10 g) were integrated to the handle to measure interaction forces between subjects' hands and handle bar and also between handle bar and the manipulator.

Three subjects seated in front of a horizontal table and the robotic system, and grasped the bar by their two hands. Wrist motions of subjects were restricted by two solid plates placing around wrists to make motion of arms similar to two-link manipulator. In the neutral position, the flexion angle of the shoulder was 90°, as the abduction angle of the shoulder was changing according to position of the handlebar. The handle bar, which was driven to four different targets, was placed to reference position (1) as shown in Fig. 2(b). As the handle bar moves between two points, the robot arm reacts against to the motion created by the subjects depending upon the specified task space stiffness.

The distance between the robot base and the subject hand was specified as 75 cm to ensure a convenient workspace for experiments. The target sets were placed to horizontal plane of the table. The displacement between reference position (Position 1) and target positions (Positions 2, 3, 4, 5) are shown in Table 1.

Using a metronome, the subjects were given a command to drive the handle bar from the reference position to the

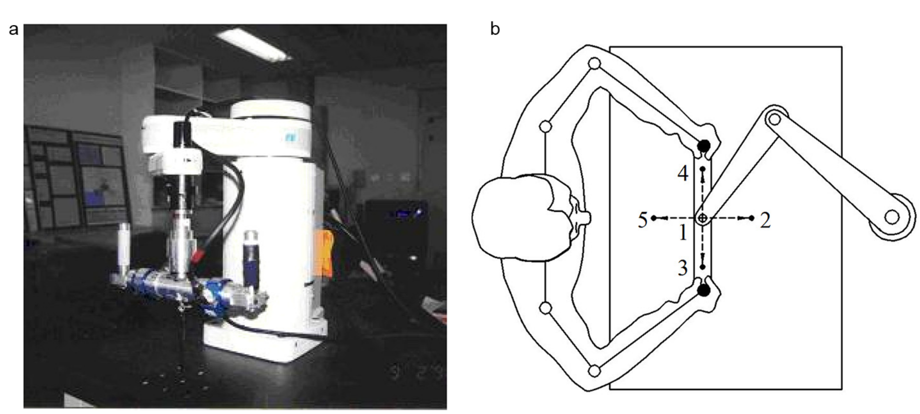


**Fig. 2 – (a) SCARA type robot used in the experiments. (b) Top view of the experimental set-up for anisometric contractions.**

**Table 1 – Directions and definitions of motion sets for anisometric contraction.**

| Direction | Definition | Distance (mm) |
|---|---|---|
| $1 \rightarrow 2$ | Forward | 50 |
| $1 \rightarrow 3$ | Rightward | 50 |
| $1 \rightarrow 4$ | Leftward | 50 |
| $1 \rightarrow 5$ | Backward | 50 |

specified target point. Each motion of handle bar performing between the reference point and a target position was divided into three phases including (i) proceed, (ii) maintain and (iii) retreat phases. Once receiving a beep signal, the subjects were directed to drive the handle bar to a specific target position. After maintaining the handle bar position for 4 s at the target point, subjects were directed to retreat the motion to the reference position with the next beep signal (Fig. 3). Force data were recorded for 2 s before proceed phase and 2 s after retreat phase, besides for 4 s during maintain phase. Three phases of the motion along rightward direction ($1 \rightarrow 3$) were given in Fig. 3. In order to overcome the potential recording errors, each trial toward the same target point was repeated 10 times. By taking the each motion direction into account, each subject performed totally 40 trials.

Position and orientation of the handle bar were detected and measured by means of the optical encoders placed on joints, which ensured to observe time-displacement graph so that a possible undesirable movement abnormalities could be detected during the measurements.

## 2.4. Signal processing and feature extraction

Recorded raw EMG signals were segmented in order to extract the time domain features. Long segment length induces high computation load, while a short one causes bias and variance in signal feature extraction. On the other hand, a segment larger than 200 ms requires overlapping to prevent failure in real-time operation [26].

In the study, recorded EMG signals were segmented via sliding windows having 500 ms time interval. Additionally, time interval between the successive windows was defined as 50 ms. Desired signal features were calculated for each segmented window.

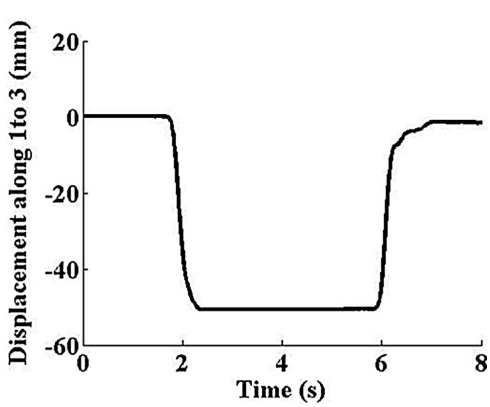


**Fig. 3 – Displacement–time profile of the joint of the handle bar for rightward phase.**

Feature extraction from EMG signal is a critical step in pattern recognition studies. The rationale behind this process is to extract useful information from a high amount of data without loosing the main character of raw signal. Time domain features are the main tools to determine the signal patterns which are indented to use in the control of prosthetics. In this study, the following time domain features were extracted.

### 2.4.1. Integrated EMG (IEMG)

Numerically, integrated EMG (IEMG) implies the summation of the EMG signal amplitude values for each segmented window. As $x_m$ denotes EMG signal in segment $m$ and, $N$ represents the number of samples (in length), IEMG is defined as follow [15]

$$\mathrm{IEMG} = \sum_{m=1}^{N} |x_m| \tag{1}$$

### 2.4.2. Root mean square (RMS)

Root mean square (RMS) is one of the most commonly used time domain features for EMG signal processing [15,27]. RMS is the envelope of the signal and calculated as

$$\mathrm{RMS} = \sqrt{\frac{1}{N}\sum_{m=1}^{N} x_m^2} \tag{2}$$

### 2.4.3. Waveform length (WL)

Waveform length (WL) implies the measure of complexity in each segment of EMG signal [15,17] and calculated as

$$\mathrm{WL} = \sum_{m=1}^{N} |\Delta x_m| \tag{3}$$

where $\Delta x_m = x_m - x_{m-1}$. WL is also cumulative length of the waveform over time segment.

Feature selection is a critical issue for EMG-based myoelectric prosthetic control, since the signal features are expected to represent the activation characteristics of the related muscle and are fed into the classification module to reflect the motor outcome.

## 2.5. Artificial neural networks

In the study, ANN that is a widely used approach for pattern recognition and classification was employed to predict the externally applied forces to each subject. The neural network structure consisted of one input layer, two hidden layers, and one output layer. The model created for the training of features that belong to isometric contractions had the layers with 21, 30, 10, and 1 neurons. For the anisometric case, neural network model had 30, 10 and 401 neurons. Log-sigmoid transfer function was employed as the transfer function. Number of the epoch was chosen 1000 for the training stage of the network. Moreover, the force values used in target set were normalized to the range between 0 and 1 to improve the classification performance of the neural network. Furthermore, training and test data were adjusted so that to reach the best fit train-test pairs for the current case. In order to carry out this, all the columns including data of different trials were employed. Leave-one-out cross-validation (LOOCV) method, which is a special kind of $k$-fold cross-validation, was performed to train the network structure and to test the accuracy of predicted results given by the same network. The network was trained using all data except only one trial and the prediction (or test) was made for that trial. In our study, LOOCV method was repeated until all of trials were used to both in training and test sessions. Accordingly, the average error was calculated by arithmetic mean of all errors of each testing trial.

Number of neurons for hidden layers was determined by trial and error approach up to obtaining the results with sufficient accuracy and certainty. According to the back-propagation feedforward approach, which was determined as the training algorithm, the weights are adjusted for each step to reduce the gradient of the cost function.

To observe if activation levels of all proximal muscles are required to be introduced to the neural network to achieve more accurate force prediction results than those obtained in the case including only one muscle, the training sessions of ANN were performed for two different variations so-called Variation I and II. In Variation I, the features belonging to all four muscles including biceps brachii, triceps brachii, pectorialis major and trapezius were used for training and testing processes. In Variation II, the networks model was only trained using EMG features of biceps brachii muscle.

A block diagram representing all process implemented from signal recording to force prediction is given in Fig. 4.

### 2.6. Assessment of the predicted force results

Force prediction results were evaluated using different methods to be able to discuss the merits and pitfalls of the characterizing performances of the features from different aspects. For isometric contraction, mean and standard deviation of predicted force values of the corresponding features for two variations were calculated. Furthermore, one-way ANOVA was implemented to determine whether the performances of the different feature extraction methods are statistically significant. The level of significance was regarded as 0.05 ($p < 0.05$).

Force prediction results in anisometric contraction were evaluated using the root mean square difference (RMSD) and the Pearson Correlation Coefficient (PCC) parameters which quantify the difference and consistency between predicted and actual forces, respectively. RMSD of forces was calculated as seen below.

$$\mathrm{RMSD} = \sqrt{\frac{\sum (f_y(n) - f_x(n))^2}{\sum (f_x(n))^2}} \tag{4}$$

where $f_x(n)$ and $f_y(n)$ represent the experimental and predicted forces, respectively. The lower RMSD values means high accuracy in prediction, namely 0.01 value of RMSD implies prediction with 1% mean error from experimental forces.

In order to measure similarity between two force-time history traces, PCC value was considered. As $C_{xy}(0)$ is the covariance, $C_{xx}(0)$ and $C_{yy}(0)$ are the autovariance of $f_x$ and $f_y$, respectively, the PCC is expressed as follows:

$$\mathrm{PCC} = \frac{C_{xy}(0)}{\sqrt{C_{xx}(0)}\sqrt{C_{yy}(0)}} \tag{5}$$

The PCC represents similarity between two data sets. If PCC value is found between two data sets as 1, it means that these two sets are completely equivalent, while 0 implies totally nonequivalent.

## 3. Results

### 3.1. Prediction results of isometric contraction

The performance of different signal features in characterizing the patients' force intentions were tested in two different data sets, namely Variation I and Variation II. Means and standard deviations (SD) of the predicted forces for the isometric case were given in Fig. 5 for Variation I and in Fig. 6 for Variation II.

In order to quantitatively evaluate the performance of features, average RMSD values between predicted and experimental forces at each force level for both variations were given in Tables 2 and 3.

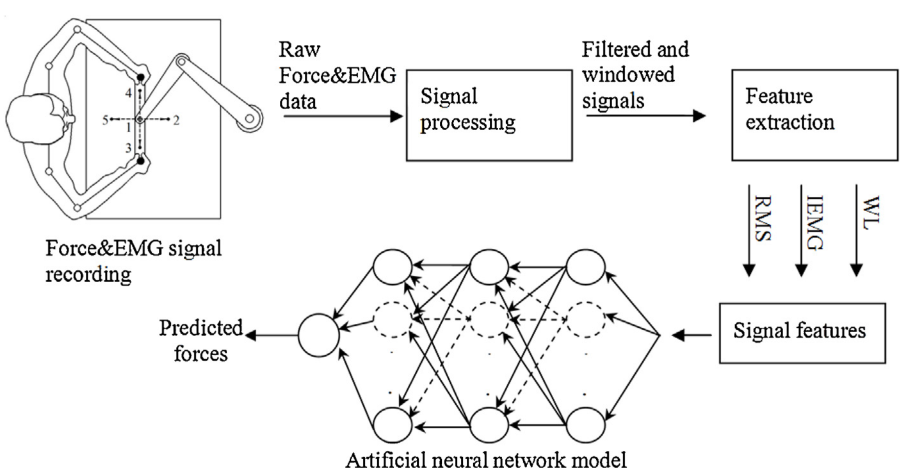


**Fig. 4 – Flow chart of the signal processing and classification phase of the study.**

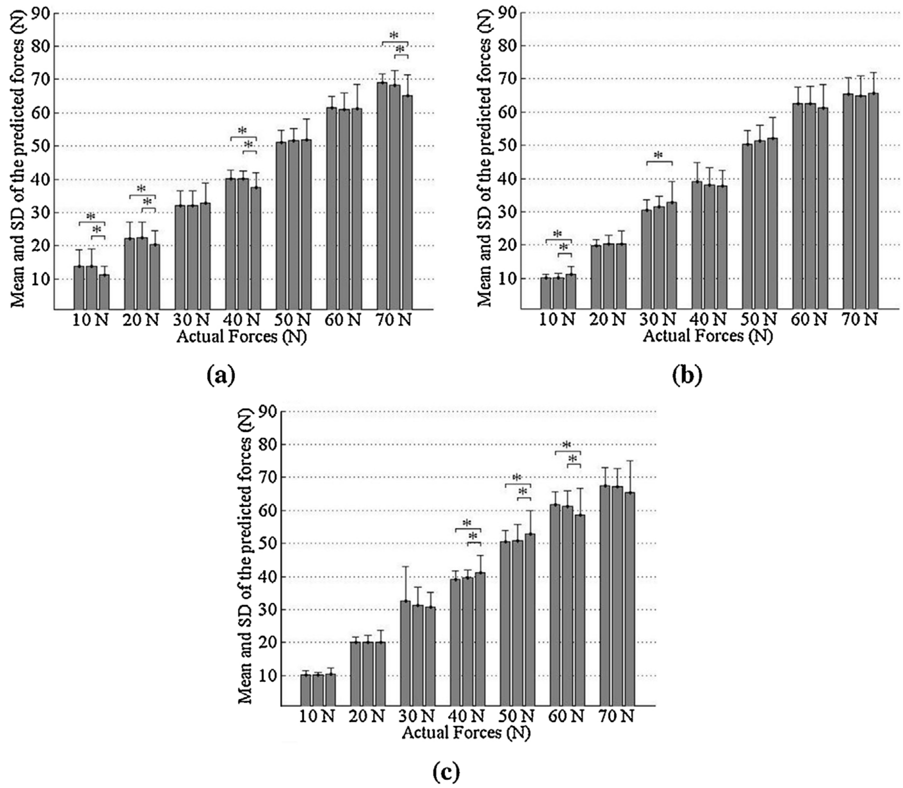


**Fig. 5 – Mean and SD of the estimated forces of Variation I for: (a) subject I; (b) subject II; and (c) subject III. Bars represent RMS, IEMG and WL features results for each force level, respectively.**

Mean RMSD values of all predicted results obtained from all subjects were given in Table 4. It can be observed from the results that minimum average RMSD value was found in case of RMS for Variation I and IEMG for Variation II ($p < 0.05$) on the other hand, highest RMSD values were obtained by WL for both variations ($p < 0.05$).

### 3.2. *Prediction results of anisometric contraction*

Representative force prediction results obtained from one of the subjects for anisometric contraction case are given for Variation I in Fig. 7. The figure shows both externally applied and predicted forces as results of pattern recognition process of the features for Variation I in which data of four muscles were used to train and test the neural network structure. The figure also contains tendency of actual applied force and predicted force results by RMS, WL and IEMG features.

In order to assess the accuracy of results, RMSD and PCC parameters were calculated for both of variations, as well. Tables 5–7 show the performance of features in prediction of forces for anisometric contractions.

It was observed from results that RMSD value was in a range of 0.08 and 0.63, 0.06 and 0.73, and 0.08 and 0.60 for RMS, IEMG, and WL features, respectively. Moreover, PCC was found in a range of 0.40 and 0.98, 0.54 and 0.98, 0.41 and 0.97 for RMS, IEMG, and WL features, respectively. Mean values of all predicted results obtained from all subjects were given in Table 8. It can be observed from the table that minimum RMSD value was obtained in case of WL for both Variation I and II ($p > 0.05$). On the other hand, highest PCC was observed in case of IEMG for both variations ($p > 0.05$).

**Table 2 – RMSD results for isometric contraction experiments in Variation I.**

| | Subject I | | | Subject II | | | Subject III | | |
|---|---|---|---|---|---|---|---|---|---|
| | RMS | IEMG | WL | RMS | IEMG | WL | RMS | IEMG | WL |
| 10 N | 0.09 | 0.07 | 0.12 | 0.02 | 0.02 | 0.11 | 0.02 | 0.06 | 0.02 |
| 20 N | 0.04 | 0.05 | 0.14 | 0.00 | 0.01 | 0.02 | 0.00 | 0.009 | 0.00 |
| 30 N | 0.06 | 0.07 | 0.11 | 0.01 | 0.05 | 0.09 | 0.08 | 0.04 | 0.02 |
| 40 N | 0.04 | 0.04 | 0.08 | 0.01 | 0.04 | 0.05 | 0.02 | 0.01 | 0.03 |
| 50 N | 0.07 | 0.07 | 0.09 | 0.00 | 0.02 | 0.04 | 0.00 | 0.01 | 0.05 |
| 60 N | 0.09 | 0.08 | 0.03 | 0.04 | 0.04 | 0.02 | 0.02 | 0.02 | 0.02 |
| 70 N | 0.02 | 0.02 | 0.08 | 0.06 | 0.07 | 0.06 | 0.03 | 0.04 | 0.06 |

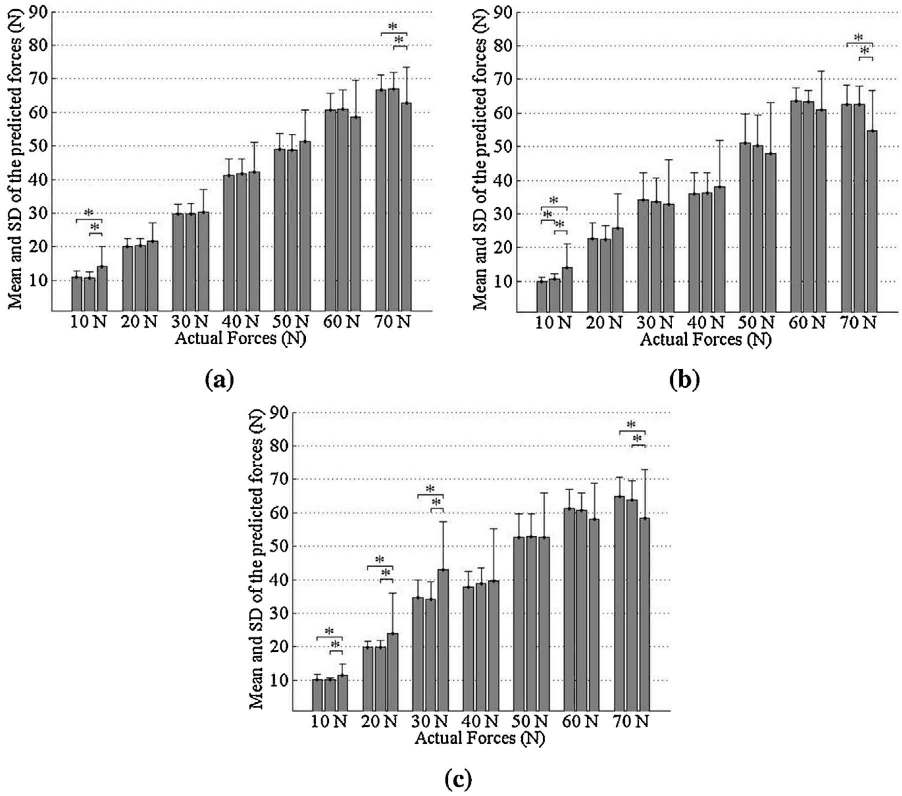


**Fig. 6 – Mean and SD of the estimated forces of Variation II for: (a) subject I; (b) subject II; and (c) subject III. For each force levels, bars represent RMS, IEMG and WL features results, respectively.**

**Table 3 – RMSD results for isometric contraction experiments in Variation II.**

| | Subject I | | | Subject II | | | Subject III | | |
|---|---|---|---|---|---|---|---|---|---|
| | RMS | IEMG | WL | RMS | IEMG | WL | RMS | IEMG | WL |
| 10 N | 0.02 | 0.02 | 0.06 | 0.12 | 0.17 | 0.80 | 0.15 | 0.07 | 0.36 |
| 20 N | 0.10 | 0.10 | 0.28 | 0.27 | 0.24 | 0.58 | 0.08 | 0.09 | 0.62 |
| 30 N | 0.09 | 0.10 | 0.22 | 0.29 | 0.26 | 0.44 | 0.23 | 0.21 | 0.63 |
| 40 N | 0.12 | 0.11 | 0.22 | 0.18 | 0.17 | 0.34 | 0.12 | 0.11 | 0.38 |
| 50 N | 0.09 | 0.09 | 0.18 | 0.17 | 0.17 | 0.30 | 0.14 | 0.14 | 0.26 |
| 60 N | 0.08 | 0.09 | 0.18 | 0.08 | 0.07 | 0.19 | 0.09 | 0.08 | 0.18 |
| 70 N | 0.07 | 0.07 | 0.18 | 0.13 | 0.13 | 0.27 | 0.10 | 0.11 | 0.26 |

**Table 4 – Mean RMSD values of the prediction results of features for all subjects in isometric case.**

| Variation I | | | Variation II | | |
|---|---|---|---|---|---|
| RMS | IEMG | WL | RMS | IEMG | WL |
| $0.03 \pm 0.02$ | $0.04 \pm 0.02$ | $0.06 \pm 0.04$ | $0.13 \pm 0.07$ | $0.12 \pm 0.06$ | $0.33 \pm 0.19$ |

## 4. Discussion

Nickolai Bernstein defined the dexterity as ''the ability to find a motor solution for any external situation, that is, to adequately solve any emerging motor problem correctly (i.e., adequately and accurately), quickly (with respect to both decision making and achieving a correct result), rationally (i.e., expediently and economically), and resourcefully (i.e., quick-wittedly and initiatively)'' [37]. Many researches have been conducted to reach a dexterous myoelectric controlled arm to ensure amputees regain their some lost fundamental motion patterns [18]. Although some encouraging and promising prosthetics were invented by researches [34], we have not seen any

**Table 5 – Prediction performance of features for motions of subject I in anisometric case.**

| Motion | Variation I | | | | | | Variation II | | | | | |
|---|---|---|---|---|---|---|---|---|---|---|---|---|
| | RMS | | IEMG | | WL | | RMS | | IEMG | | WL | |
| | RMSD | PCC | RMSD | PCC | RMSD | PCC | RMSD | PCC | RMSD | PCC | RMSD | PCC |
| $1 \rightarrow 2$ | 0.08 | 0.77 | 0.06 | 0.79 | 0.19 | 0.65 | 0.12 | 0.61 | 0.24 | 0.74 | 0.17 | 0.54 |
| $1 \rightarrow 3$ | 0.32 | 0.76 | 0.37 | 0.77 | 0.18 | 0.83 | 0.33 | 0.79 | 0.25 | 0.79 | 0.27 | 0.76 |
| $1 \rightarrow 4$ | 0.23 | 0.61 | 0.35 | 0.74 | 0.24 | 0.63 | 0.32 | 0.76 | 0.39 | 0.79 | 0.35 | 0.71 |
| $1 \rightarrow 5$ | 0.09 | 0.87 | 0.31 | 0.65 | 0.24 | 0.86 | 0.16 | 0.79 | 0.18 | 0.82 | 0.16 | 0.70 |

**Table 6 – Prediction performance of features for motions of subject II in anisometric case.**

| Motion | Variation I | | | | | | Variation II | | | | | |
|---|---|---|---|---|---|---|---|---|---|---|---|---|
| | RMS | | IEMG | | WL | | RMS | | IEMG | | WL | |
| | RMSD | PCC | RMSD | PCC | RMSD | PCC | RMSD | PCC | RMSD | PCC | RMSD | PCC |
| $1 \rightarrow 2$ | 0.12 | 0.98 | 0.42 | 0.89 | 0.08 | 0.97 | 0.23 | 0.98 | 0.14 | 0.98 | 0.11 | 0.75 |
| $1 \rightarrow 3$ | 0.29 | 0.67 | 0.45 | 0.79 | 0.32 | 0.61 | 0.63 | 0.73 | 0.55 | 0.75 | 0.47 | 0.62 |
| $1 \rightarrow 4$ | 0.48 | 0.44 | 0.47 | 0.74 | 0.39 | 0.59 | 0.56 | 0.40 | 0.73 | 0.43 | 0.60 | 0.41 |
| $1 \rightarrow 5$ | 0.16 | 0.71 | 0.29 | 0.66 | 0.23 | 0.71 | 0.21 | 0.69 | 0.34 | 0.76 | 0.25 | 0.50 |

**Table 7 – Prediction performance of features for motions of subject III in anisometric case.**

| Motion | Variation I | | | | | | Variation II | | | | | |
|---|---|---|---|---|---|---|---|---|---|---|---|---|
| | RMS | | IEMG | | WL | | RMS | | IEMG | | WL | |
| | RMSD | PCC | RMSD | PCC | RMSD | PCC | RMSD | PCC | RMSD | PCC | RMSD | PCC |
| $1 \rightarrow 2$ | 0.30 | 0.77 | 0.16 | 0.74 | 0.31 | 0.60 | 0.33 | 0.62 | 0.31 | 0.62 | 0.43 | 0.72 |
| $1 \rightarrow 3$ | 0.39 | 0.62 | 0.24 | 0.54 | 0.28 | 0.68 | 0.29 | 0.85 | 0.30 | 0.70 | 0.30 | 0.67 |
| $1 \rightarrow 4$ | 0.48 | 0.70 | 0.19 | 0.93 | 0.26 | 0.63 | 0.19 | 0.77 | 0.17 | 0.74 | 0.11 | 0.74 |
| $1 \rightarrow 5$ | 0.25 | 0.91 | 0.22 | 0.74 | 0.31 | 0.89 | 0.29 | 0.85 | 0.24 | 0.85 | 0.25 | 0.60 |

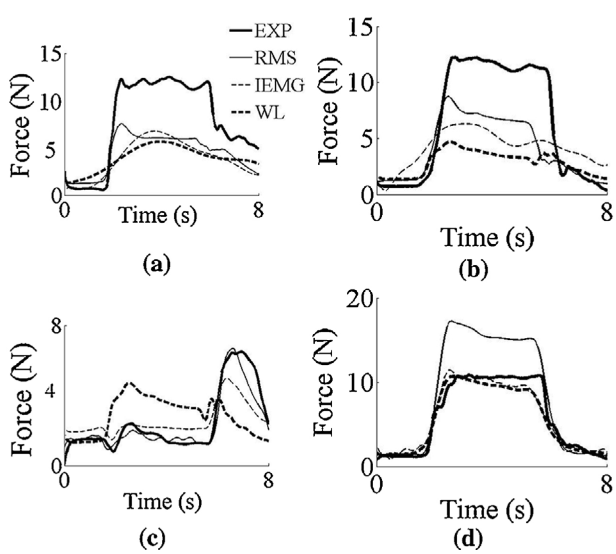


**Fig. 7 – A representative comparison of the actual and the predicted forces created during a subject motion pattern for Variation I: (a) forward: $1 \rightarrow 2$; (b) rightward: $1 \rightarrow 3$; (c) leftward: $1 \rightarrow 4$; and (d) backward: $1 \rightarrow 5$.**
**EXP: experimental, RMS: root mean square, IEMG: integrated EMG, WL: waveform length.**

**Table 8 – Mean values of the prediction results of features for all subjects in anisometric case.**

| | Variation I | | Variation II | |
|---|---|---|---|---|
| | RMSD | PCC | RMSD | PCC |
| RMS | $0.27 \pm 0.14$ | $0.73 \pm 0.15$ | $0.30 \pm 0.15$ | $0.74 \pm 0.15$ |
| IEMG | $0.29 \pm 0.13$ | $0.75 \pm 0.10$ | $0.32 \pm 0.17$ | $0.75 \pm 0.13$ |
| WL | $0.25 \pm 0.08$ | $0.72 \pm 0.13$ | $0.29 \pm 0.15$ | $0.64 \pm 0.11$ |

dexterous prosthetic arm that is highly functional, easy to use and cost efficient. Beside the mechanical and spatial limitations, one challenging problem researchers are also facing with is that how to control intuitively such prosthetics with accuracy. Human arm prostheses have limitations regarding controlling specific motion patterns consistently and seamlessly. Sending control signals created from the own body of the user to actuators to create any desired motion is still mainly a critical issue. This kind of control highly depends upon gathering the clear and usable outcome from classifier which uses myoelectric signal features and characteristics. Thus, selection of appropriate EMG feature classification and pattern recognition techniques plays an important role in dexterous control of human arm prostheses.

For isometric contraction, by taking average RMSD values into account it can be observed that RMS and IEMG are superior to WL (Table 4) for Variation I ($p < 0.05$) and II ($p < 0.05$). If each force level is considered individually it can be deduced that nearly for half of the all force levels, there is significant difference between WL and RMS/IEMG prediction results (Figs. 5 and 6). Additionally, considering RMSD results for isometric contraction in Tables 2 and 3, maximum number of predictions, which is the closest to the actual force levels, is provided by RMS feature. Besides the fact that RMS seems to be successful in estimation of forces, the performance of IEMG is not negligible due to the fact that, for both of variations, there are many predictions that RMS and IEMG provide the similar results. For most of the force levels, significant difference between RMS and IEMG results were not found. However, RMS provided more numbers of accurate results in terms of quantification. Back to WL performance, for two variations, the feature showed a worse prediction outputs than other two features which suggests that WL feature is not preferable for force estimation for isometric contractions. As for comparison of the variations, Variation I includes more accurate results than Variation II for all features ($p < 0.05$). Despite more data increased the complexity of networks and resulted in more computational burden, it seems that the variation including data of four muscles ensured a more successful prediction of the forces than the one including only one muscle. The rationale behind this finding could be explained by the proposition which suggests that the motion generation or resistances of muscles are driven by various combinations of the synergistic effects among the activated muscles. Also, co-contraction of muscles is another mechanism that specifies the inherent muscle coordination during performing some certain motor tasks.

For anisometric contractions, prediction results of both variations show that actual time-varying force trends could be reached by performing time domain features. According to mean RMSD results presented in Table 8, WL provided slightly more accurate results than RMS and IEMG ($p > 0.05$). Average RMSD values of prediction results of RMS and IEMG are very close to each others, as 0.27, and 0.31 obtained from RMS for variation I and variation II, respectively, and for the same cases 0.29 and 0.32 were obtained by IEMG. On the other hand, PCC is another critical parameter to measure and evaluate the performance of a signal feature. Considering mean PCC results of anisometric case shown in Table 8, IEMG showed a better force prediction characterization than RMS and WL ($p > 0.05$). Mean PCC values of RMS and IEMG were found as 0.73, and 0.75, respectively, for Variation I, and 0.74 and 0.75 for Variation II. It is clear that RMS and IEMG showed a satisfactory performance in terms of both RMSD and PCC parameters. It can be claimed that both features provided reasonable prediction accuracy. In terms of mean PCC values, especially for Variation II, WL feature predicted force results with less accuracy than those made by RMS and IEMG ($p > 0.05$). Therefore, it can be deduced that WL feature showed limited performance for anisometric case in terms of the illustrating the similarity to the experimental force-time history.

Although the prediction results demonstrate an acceptable performance in terms of characterizing the force generation intentions of the subjects, to create a set of rules regarding establishing an optimum ANN structure is still a challenging tasks [38]. Empirical nature of model development is one of the most important disadvantages of neural networks. Structure of input data and labeling of target set are also influential on the classification results due to clear and meaningful selection of data is closely related to the prediction performance of the classifier. The trade off between accuracy and computational cost, which affects closely the duration of the analysis, should also be taken into account for each case. Moreover, designing complex networks structure does not guarantee obtaining accurate prediction results due to proneness to overfitting.

## 5. Conclusion

In this study, different widely used time domain features of EMG signals including root mean square (RMS), integrated EMG (IEMG), and waveform length (WL) were comparatively evaluated for the prediction of externally applied forces to human hands. Extracted features from EMG signals were classified using artificial neural networks (ANN) to predict the targeted forces. For this scope, an ANN structure was built and trained with EMG feature data set to reach experimentally applied force values. It was concluded that RMS and IEMG features shows a consistent and satisfactory signal characterization performance. In addition, for RMS and IEMG features, it was not found considerable difference between the prediction results of Variation I and II which suggests that an equivalent performance can be achieved with less number of muscles instead of recruiting many EMG data from many muscles. Hence, motor intentions of amputees may be reflected with limited number of muscles in prosthetic limbs. The present study is expected to be useful for further studies for investigation and evaluation of the relationships between different signal features and various motion patterns. The obtained results are anticipated to contribute to the classification process of EMG signal and motion control approaches of powered human arm prosthetics.

## Acknowledgements

The authors would like to thank Prof. Dr. Mehmet Baris BASLO for his support and motivation in conducting the experiments. This research was supported by The Research Fund of the Istanbul University, Project No. BEK-2016-22500 and 46583.

## REFERENCES

[1] De Luca CJ. Physiology and mathematics of myoelectric signals. IEEE Trans Biomed Eng 1979;26(6):313–25.
[2] Young AJ, Smith LH, Rouse EJ, Hargrove LJ. Classification of simultaneous movements using surface EMG pattern recognition. IEEE Trans Biomed Eng 2013;60(5):1250–8.
[3] Farina D, Jiang N, Rehbaum H, Holobar A, Graimann B, Aszmann OC. The extraction of neural information from the surface EMG for the control of upper-limb prostheses: emerging avenues and challenges. IEEE Trans Neural Syst Rehabil Eng 2014;22(4):797–809.

[4] Muceli S, Jiang N, Farina D. Multichannel surface EMG based estimation of bilateral hand kinematics during movements at multiple degrees of freedom. Proc. 32nd Annual International Conference of the IEEE EMBS; 2010.
[5] Morita S, Shibata K, Zheng XZ, Ito K. Prosthetic hand control based on torque estimation from EMG signals. Proc. International Conference on Intelligent Robots and Systems; 2000.
[6] Scheme E, Englehart K. Electromyogram pattern recognition for control of powered upper-limb prostheses: state of the art and challenges for clinical use. J Rehabil Res Dev 2011;48(6):643–59.
[7] Resnik L, Etter K, Klinger SL, Kambe CR. Using virtual reality environment to facilitate training with advanced upper-limb prosthesis. J Rehabil Res Dev 2011;48(6):707–18.
[8] Huang Y, Englehart KB, Hudgins B, Chan ADC. A Gaussian mixture model based classification scheme for myoelectric control of powered upper limb prostheses. IEEE Trans Biomed Eng 2005;52(11):1801–11.
[9] Kyberd PJ, Lemaire ED, Scheme E, MacPhail C, Goudreau L, Bush G, et al. Two-degree-of-freedom powered prosthetic wrist. J Rehabil Res Dev 2011;48(6):609–17.
[10] Cipriani C, Zaccone F, Micera S, Carrozza MC. On the shared control of an EMG-controlled prosthetic hand: analysis of user–prosthesis interaction. IEEE Trans Robot 2008;24(1):170–84.
[11] Guo X, Yang P, Li Y, Yan W. The SEMG analysis for the lower limb prosthesis using wavelet transformation. Proc. 26th Annual International Conference of the IEEE; 2004.
[12] Roman-Liu D, Tokarski T. EMG of arm and forearm muscle activities with regard to handgrip force in relation to upper limb location. Acta Bioeng Biomech 2002;4(2):33–47.
[13] Arslan YZ, Adli MA, Akan A, Baslo MB. Prediction of externally applied forces to human hands using frequency content of surface EMG signals. Comput Methods Programs Biomed 2010;98(1):36–44.
[14] Corbett EA, Perreault EJ, Kuiken TA. Comparison of electromyography and force as interfaces for prosthetic control. J Rehabil Res Dev 2011;48(6):629–41.
[15] Phinyomark A, Phukpattaranont P, Limsakul C. Feature reduction and selection for EMG signal classification. Expert Syst Appl 2012;39(8):7420–31.
[16] Oskoei MA, Hu H. Myoelectric control systems – a survey. Biomed Signal Process Control 2007;2(4):275–94.
[17] Phinyomark A, Quaine F, Charbonnier S, Serviere C, Tarpin-Bernard F, Laurillau Y. Feature extraction of the first difference of EMG time series for EMG pattern recognition. Comput Methods Programs Biomed 2014;117(2):247–56.
[18] Zecca M, Micera S, Carozza MC, Dario P. Control of multifunctional prosthetic hands by processing the electromyographic signal. Crit Rev Biomed Eng 2002;30(4–6):459–85.
[19] Hudgins B, Parker P, Scott RN. A new strategy for multifunction myoelectric control. IEEE Trans Biomed Eng 1993;40(1):82–94.
[20] Ajiboye AB, Weir RF. A heuristic fuzzy logic approach to EMG pattern recognition for multifunctional prosthesis control. IEEE Trans Neural Syst Rehabil Eng 2005;13(3):280–91.
[21] Jun-Uk C, Inhyuk M, Mu-Seong M. A real-time EMG pattern recognition system based on linear-nonlinear feature projection for a multifunction myoelectric hand. IEEE Trans Biomed Eng 2006;53(11):2232–9.
[22] Li G, Schultz AE, Kuiken TA. Quantifying pattern recognition-based myoelectric control of multifunctional transradial prostheses. IEEE Trans Neural Syst Rehabil 2010;18(2):185–92.
[23] Lucas MF, Gaufriau A, Pascual S, Doncarli C, Farina D. Multi-channel surface EMG classification using support vector machines and signal-based wavelet optimization. Biomed Signal Process Control 2008;3(2):169–74.
[24] Oskoei MA, Hu H. Support vector machine-based classification scheme for myoelectric control applied to upper limb. IEEE Trans Biomed Eng 2008;55(8):1956–65.
[25] Yoshikawa M, Mikawa M, Tanaka K. Real-time hand motion estimation using EMG signals with support vector machines. Proc. SICE-ICASE International Joint Conference; 2006.
[26] Alkan A, Gunay M. Identification of EMG signals using discriminant analysis and SVM classifier. Expert Syst Appl 2012;39(1):44–7.
[27] Kim KS, Choi HH, Moon CS, Mun CW. Comparison of k-nearest neighbor, quadratic discriminant and linear discriminant analysis in classification of electromyogram signals based on the wrist-motion directions. Curr Appl Phys 2011;11(3):740–5.
[28] Chan FHY, Yong-Sheng Y, Lam FK, Yuan-Ting Z. Fuzzy EMG classification for prosthesis control. IEEE Trans Rehabil Eng 2000;8(3):305–11.
[29] Micera S, Sabatini AM, Dario P, Rossi B. A hybrid approach to EMG pattern analysis for classification of arm movements using statistical and fuzzy techniques. Med Eng Phys 1999;21(5):303–11.
[30] Gallant PJ, Morin EL, Peppard LE. Feature-based classification of myoelectric signals using artificial neural networks. Med Biol Eng Comput 1998;36(4):485–9.
[31] Kuribayashi K, Shimizu S, Okimura K, Taniguchi T. A discrimination system using neural network for EMG-controlled prostheses-Integral type of EMG signal processing. Proc. IEEE/RSJ International Conference on Intelligent Robots and Systems; 1993.
[32] Baspinar U, Varol HS, Senyurek VY. Performance comparison of artificial neural network and Gaussian mixture model in classifying hand motions by using sEMG signals. Biocybern Biomed Eng 2013;33(1):33–45.
[33] Hiraiwa A, Shimohara K, Tokunaga Y. EMG pattern analysis and classification by neural network. Proc. IEEE International Conference on Systems, Man and Cybernetics; 1989.
[34] Liu MM, Herzog W, Savelberg HHCM. Dynamic muscle force predictions from EMG: an artificial neural network approach. J Electromyogr Kinesiol 1999;9(6):391–400.
[35] Hermens H, Freriks B, Merletti R, Stegeman D, Block J, Rau G, et al. SENIAM: European recommendations for surface electromyography. Enschede, Holland: Roessingh Research and Development; 1999 (ISBN 90-75452-15-2).
[36] Qi L, Wakeling J, Grange S, Ferguson-Pell M. Changes in surface electromyography signals and kinetics associated with progression of fatigue at two speeds during wheelchair propulsion. J Rehabil Res Dev 2012;49(1):23–34.
[37] Bernstein NA. In: Latash ML, Turvey MT, editors. On dexterity and its development. Hillsdale, NJ: Lawrence Erlbaum Associates; 1996. p. 3–244.
[38] Demir U, Kocaoğlu S, Akdoğan E. Human impedance parameter estimation using artificial neural network for modelling physiotherapist motion. Biocybern Biomed Eng 2016;36:318–26.